JOURNAL OF THEORETICAL AND APPLIED MECHANICS
49, 3, pp. 641-664, Warsaw 2011

VIBRATION ANALYSIS OF A TRIMORPH PLATE FOR OPTIMISED DAMAGE MITIGATION

Akuro Big-Alabo
University of Port Harcourt, Department of Mechanical Engineering, Rivers State, Nigeria e-mail: bigalabo@yahoo.com

Matthew P. Cartmell
University of Glasgow, School of Engineering, Systems, Power and Energy Research Division, Glasgow, Scotland, UK; e-mail: matthew.cartmell@glasgow.ac.uk

The dynamic response of a viscously damped rectangular trimorph plate subjected to a sinusoidally distributed load was investigated for simply-supported boundary conditions. The governing equation for the nonlinear deflection of the plate, which is first introduced in this paper, was derived based on the classical plate theory (CPT) and the classical laminate theory (CLT). The governing equation was solved using the Navier method and direct numerical integration. Optimised time-domain response plots for a trimorph plate made up of aluminium (Al), polyvinylidene fluoride (PVDF) and lead zirconate titanate (PZT) layers revealed that only three out of the six possible layer configurations are necessary for determining the best layer-stacking. In determining the best layer-stacking for the optimised dynamic response, three factors were considered namely: the stiffness, natural frequency and damping constant. Both of the Al/PVDF/PZT or Al/PZT/PVDF configurations were found to produce the best response qualities i.e. high elastic stiffness, high natural frequency and low viscous damping. Frequency-domain plots were generated to compare the nonlinear and linear responses and it was discovered that the effect of the nonlinearity predictably reduces the natural frequency of the trimorph plate. This study can be applied to the analysis of optimised damage mitigation of intelligent car bodies and safety critical structures which are subject to potentially destructive loading conditions.

Key words: trimorph, layer-stacking, reference layer, classical plate theory

1. Introduction

In recent times, research on the vibration of plates has inclined towards laminated plates. This is because desirable operational qualities of materials such

as strength, stiffness, low-weight, wear resistance and acoustical insulation etc. can be achieved by using laminates (Jones, 1999), especially composite laminates.

Lee (1990) developed the theory of laminated piezoelectric plates (TLPP) for the design of distributed sensor/actuators. He developed the governing equations and the reciprocal relationships of distributed piezoelectric sensors and actuators for the laminated piezoelectric plate. Liew *et al.* (2004) studied the vibration control of a laminated composite plate with piezoelectric sensor/actuator patches. They developed an algorithm with which they studied the dynamic response of the laminated plate and illustrated the effect of stacking and positioning of sensor/actuator patches on the response of the laminated plate. Zenkour (2004) examined the response of cross-ply laminated plates subject to thermo-mechanical loading. He demonstrated the influence of material anisotropy and stacking sequence, among others, on the thermally induced response of the plate. Ganilova and Cartmell (2010) explored the vibration control of a shape memory alloy (SMA) integrated laminated sandwich plate by means of a controllable activation strategy. Their vibration model contains time-dependent coefficients and hence requires careful selection of input conditions to obtain practically realistic results.

In the literature, the word *trimorph* has been used to describe the kind of laminate studied. For instance, Craciunescu *et al.* (2005) used the word trimorph to denote a substrate sandwiched between two film layers. The substrate used was silicon while the films were Nickel-Titanium (NiTi) shape memory alloy (SMA). Chang and Lin (2003) in the vibration analysis of a ring used the word trimorph to represent a three-layer ring with an elastic material (substrate) laminated in between two piezoelectric layers. Papila *et al.* (2008) making reference to the configuration described by Chang and Lin considered it as a *bimorph*. Roytburd *et al.* (1998) and Erturk and Inman (2008) used the same architecture to mean bimorph just as Papila *et al.*. Hence, there is no standard definition as to the use of the word trimorph. In this study, the word trimorph is used in a general sense to mean a three-layer laminate. Also, *layer-stacking* is used to mean the different possible permutations of the layers, which are obviously six for a three-layer laminate.

This paper investigates the dynamic response of a trimorph plate subjected to forced vibration. Vibration analysis for nonlinear and linear responses for the different layer-stackings has been undertaken in order to determine the layer-stacking that produces the best desirable material characteristics for an optimised response. In developing the governing equations, classical laminate theory (CLT) has been applied and the governing equations were solved to

simulate the trimorph plate response using a combined solution of the Navier method and direct integration in the time domain using Mathematica^{TM}.

2. Governing equations of the trimorph plate

The system (trimorph plate) whose dynamic behaviour is modelled is a rectangular plate having three layers bonded adhesively together so that there is negligible relative motion between the layers. The layers are of different materials and all the material properties are isotropic. The system is simply supported on all four edges, under-damped and subjected to a sinusoidally distributed load. Figure 1 provides a sketch of the system. The layers in Fig. 1 have different shading patterns suggesting that they are made of different materials.

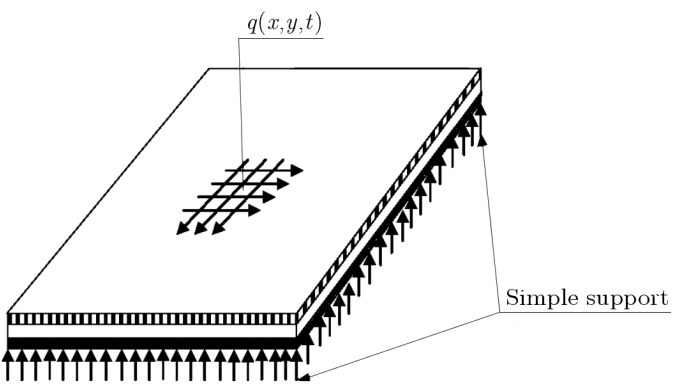

Fig. 1. Diagrammatic description of the system

The trimorph plate is modelled as a thin plate and therefore all the assumptions for modelling thin plates apply. The equations of motion for a thin rectangular plate subject to membrane force based on the classical plate theory (CPT) are derived in Whitney (1987) and are shown below

$$\begin{aligned}&\frac{\partial^2 M_x}{\partial x^2}+2\frac{\partial^2 M_{xy}}{\partial x\partial y}+\frac{\partial^2 M_y}{\partial y_2}\\&\quad=\rho h\frac{\partial^2 w}{\partial t^2}+c\frac{\partial w}{\partial t}-q(x,y,t)+N_x\frac{\partial^2 w}{\partial x^2}+2N_{xy}\frac{\partial^2 w}{\partial x\partial y}+N_y\frac{\partial^2 w}{\partial y^2}\end{aligned}\tag{2.1}$$

and

$$\frac{\partial N_y}{\partial y}+\frac{\partial N_{xy}}{\partial x}=\rho h\frac{\partial^2 v}{\partial t^2}\qquad\qquad\frac{\partial N_x}{\partial x}+\frac{\partial N_{xy}}{\partial y}=\rho h\frac{\partial^2 u}{\partial t^2}\tag{2.2}$$

In equation (2.1), the terms on the left hand side represent the effect of bending moments on the lateral displacement, while the last three terms on the right hand side represent the effect of membrane forces on the lateral displacement. The first three terms on the right hand side are the lateral acceleration, the classical linear viscous damping force, and the excitation force acting on the plate respectively. The excitation function is a time-dependent sinusoidally distributed load and can be expressed as

$$q(x,y,t) = q(t)\sin\frac{\pi x}{a}\sin\frac{\pi y}{b} \tag{2.3}$$

where a and b are the in-plane dimensions of the plate and $q(t)$ is a time-variant forcing function. For the purpose of this study, $q(t)$ is assumed to be a sinusoidal function with amplitude q i.e. $q(t) = q\sin(\omega t)$. In equations (2.2), the left hand side represents the effect of membrane forces while the right hand side represents the accelerations in the in-plane directions.

The formulation of the classical laminate theory (CLT) is extensively discussed in some text on composites (Vinson and Sierakowski, 2004; Reddy, 2004; Voyiadjis and Kattan, 2005 etc). Lee (1990) developed the TLPP using the CLT. Lu and Li (2009) compared results obtained by various plate theories, including CLT, and the CLT results were in good agreement with other theories. Ganilova and Cartmell (2010) applied a dynamic model based on CLT in the modelling and vibration control of an active sandwich plate.

For the general case of an unsymmmetric laminate with isotropic layers, the constitutive laminate equations based on the CLT are given by Jones (1999) as

$$\begin{Bmatrix} N_x \\ N_y \\ N_{xy} \end{Bmatrix} = \begin{bmatrix} A_{11} & A_{12} & 0 \\ A_{12} & A_{11} & 0 \\ 0 & 0 & A_{66} \end{bmatrix} \begin{Bmatrix} \varepsilon_x^0 \\ \varepsilon_y^0 \\ \varepsilon_{xy}^0 \end{Bmatrix} + \begin{bmatrix} B_{11} & B_{12} & 0 \\ B_{12} & B_{11} & 0 \\ 0 & 0 & B_{66} \end{bmatrix} \begin{Bmatrix} k_x^0 \\ k_y^0 \\ k_{xy}^0 \end{Bmatrix}$$

$$\begin{Bmatrix} M_x \\ M_y \\ M_{xy} \end{Bmatrix} = \begin{bmatrix} B_{11} & B_{12} & 0 \\ B_{12} & B_{11} & 0 \\ 0 & 0 & B_{66} \end{bmatrix} \begin{Bmatrix} \varepsilon_x^0 \\ \varepsilon_y^0 \\ \varepsilon_{xy}^0 \end{Bmatrix} + \begin{bmatrix} D_{11} & D_{12} & 0 \\ D_{12} & D_{11} & 0 \\ 0 & 0 & D_{66} \end{bmatrix} \begin{Bmatrix} k_x^0 \\ k_y^0 \\ k_{xy}^0 \end{Bmatrix} \tag{2.4}$$

where $\{N\}$, $\{M\}$, $\{\varepsilon\}$, and $\{k\}$ are the membrane force, bending moment, elastic strain, and surface curvature vectors, respectively. $[A_{ij}]$, $[B_{ij}]$ and $[D_{ij}]$ are the extension, bending-extension coupling, and bending stiffness matrices respectively, and the elements of the matrices are given by

$$[A_{ij}] = \sum_{k=1}^{N} \overline{Q}_{ijk}(z_k - z_{k-1}) \qquad [B_{ij}] = \frac{1}{2}\sum_{k=1}^{N} \overline{Q}_{ijk}(z_k^2 - z_{k-1}^2)$$
$$[D_{ij}] = \frac{1}{3}\sum_{k=1}^{N} \overline{Q}_{ijk}(z_k^3 - z_{k-1}^3) \tag{2.5}$$

where $\overline{Q}_{ijk}$ is the transformed reduced stiffness of the kth layer of the laminate, k is the layer index, and N is the total number of layers. The kth layer is bounded by surfaces at z_k and z_{k-1} at the top and bottom respectively. For the case of an unsymmetric laminate considered here, $\overline{Q}_{ijk}$ is related to the material properties of the kth layer as shown in equations (2.6) below

$$(\overline{Q}_{11})_k = (\overline{Q}_{22})_k = \frac{E_k}{1-\nu_k^2} \qquad (\overline{Q}_{16})_k = (\overline{Q}_{26})_k = 0$$
$$(\overline{Q}_{12})_k = \frac{\nu_k E_k}{1-\nu_k^2} \qquad (\overline{Q}_{66})_k = \frac{E_k}{2(1+\nu_k)} \tag{2.6}$$

By substituting equations (2.4) in equations (2.1) and (2.2) and applying Kirchhoff's strain-displacement relationships (Voyiadjis and Kattan, 2005), the following equations are obtained

$$\begin{aligned}
&B_{11}\frac{\partial^3 u}{\partial x^3} + (B_{12}+2B_{66})\frac{\partial^3 u}{\partial x \partial y^2} + (B_{12}+2B_{66})\frac{\partial^3 v}{\partial x^2 \partial y} + B_{11}\frac{\partial^3 v}{\partial y^3} \\
&\quad -\Big[D_{11}\frac{\partial^4 w}{\partial x^4} + 2(D_{12}+2D_{66})\frac{\partial^4 w}{\partial x^2 \partial y^2} + D_{11}\frac{\partial^4 w}{\partial y^4}\Big] \\
&\quad = \rho h\frac{\partial^2 w}{\partial t^2} + c\frac{\partial w}{\partial t} - q(x,y,t) + \Big(A_{11}\frac{\partial^2 w}{\partial x^2} + A_{12}\frac{\partial^2 w}{\partial y^2}\Big)\frac{\partial u}{\partial x} \\
&\quad +\Big(A_{12}\frac{\partial^2 w}{\partial x^2} + A_{11}\frac{\partial^2 w}{\partial y^2}\Big)\frac{\partial v}{\partial y} + B_{11}\Big[\Big(\frac{\partial^2 w}{\partial y^2}\Big)^2 + \Big(\frac{\partial^2 w}{\partial x^2}\Big)^2\Big] \\
&\quad +2A_{66}\Big(\frac{\partial u}{\partial y} + \frac{\partial v}{\partial x}\Big)\frac{\partial^2 w}{\partial x \partial y} - 4B_{66}\Big(\frac{\partial^2 w}{\partial x \partial y}\Big)^2 \qquad (2.7)\\
&A_{66}\frac{\partial^2 v}{\partial x^2} + A_{11}\frac{\partial^2 v}{\partial y^2} + (A_{12}+A_{66})\frac{\partial^2 u}{\partial x \partial y} - B_{11}\frac{\partial^3 w}{\partial y^3} \\
&\quad -(B_{12}+2B_{66})\frac{\partial^3 w}{\partial x^2 \partial y} = \rho h\frac{\partial^2 v}{\partial t^2} \\
&A_{11}\frac{\partial^2 u}{\partial x^2} + A_{66}\frac{\partial^2 u}{\partial y^2} + (A_{12}+A_{66})\frac{\partial^2 v}{\partial x \partial y} - B_{11}\frac{\partial^3 w}{\partial x^3} \\
&\quad +(B_{12}-2B_{66})\frac{\partial^3 w}{\partial x \partial y^2} = \rho h\frac{\partial^2 u}{\partial t^2}
\end{aligned}$$

Equations (2.7) are PDEs in more than one independent variables, which can be reduced to ODEs using the Navier Method (Ganilova and Cartmell, 2010; Zak *et al.*, 2003). For a time-variant sinusoidally distributed load as expressed in equation (2.3), the appropriate solution for the displacements based on the Navier method can be deduced from Ganilova and Cartmell (2010) as follows

$$\begin{aligned} u(x,y,t) &= u(t)\sin\frac{\pi x}{a}\sin\frac{\pi y}{b} \\ v(x,y,t) &= v(t)\sin\frac{\pi x}{a}\sin\frac{\pi y}{b} \\ w(x,y,t) &= w(t)\sin\frac{\pi x}{a}\sin\frac{\pi y}{b} \end{aligned} \tag{2.8}$$

Substituting equations (2.8) and their derivatives into equations (2.7) and simplifying the resulting expressions, we obtain

$$\begin{aligned} &-\pi^3\Big(\frac{B_{11}}{a^3}+\frac{B_{12}+2B_{66}}{ab^2}\Big)u(t)\cot\frac{\pi x}{a}-\pi^3\Big(\frac{B_{11}}{b^3}+\frac{B_{12}+2B_{66}}{a^2b}\Big)v(t)\cot\frac{\pi y}{b} \\ &\quad-\pi^4\Big(\frac{D_{11}}{a^4}+\frac{2(D_{12}+2D_{66})}{a^2b^2}+\frac{D_{11}}{b^4}\Big)w(t)-2\pi^3A_{66}\Big(\frac{1}{ab^2}u(t)\cot\frac{\pi y}{b} \\ &\quad+\frac{1}{a^2b}v(t)\cot\frac{\pi x}{a}\Big)w(t)\cos\frac{\pi x}{a}\cos\frac{\pi y}{b} \\ &\quad=\rho h\ddot{w}+c\dot{w}-q(t)-\pi^3\Big(\frac{A_{11}}{a^3}+\frac{A_{66}}{a^2b}\Big)u(t)v(t)\cos\frac{\pi x}{a}\sin\frac{\pi y}{b} \\ &\quad-\pi^3\Big(\frac{A_{12}}{a^2b}+\frac{A_{11}}{b^3}\Big)v(t)w(t)\sin\frac{\pi x}{a}\cos\frac{\pi y}{b}+\pi^4\Big[B_{11}\Big(\frac{1}{b^4}+\frac{1}{a^4}\Big)\sin\frac{\pi x}{a}\sin\frac{\pi y}{b} \\ &\quad-4B_{66}\frac{1}{a^2b^2}\cot\frac{\pi x}{a}\cot\frac{\pi y}{b}\cos\frac{\pi x}{a}\cos\frac{\pi y}{b}\Big][w(t)]^2 \\ &\frac{\pi}{ab}(A_{12}+A_{66})u(t)\cot\frac{\pi x}{a}\cot\frac{\pi y}{b}-\pi^2\Big(\frac{A_{66}}{a^2}+\frac{A_{11}}{b^2}\Big)v(t) \\ &\quad-\pi^3\Big(\frac{B_{11}}{b^3}-\frac{B_{12}+2B_{66}}{a^2b}\Big)w(t)\cot\frac{\pi y}{b}=\rho h\ddot{v} \\ &-\pi^2\Big(\frac{A_{11}}{a^2}+\frac{A_{66}}{b^2}\Big)u(t)+\frac{\pi}{ab}(A_{12}+A_{66})v(t)\cot\frac{\pi x}{a}\cot\frac{\pi y}{b} \\ &\quad+\pi^3\Big(\frac{B_{11}}{b^3}-\frac{B_{12}-2B_{66}}{ab^2}\Big)w(t)\cot\frac{\pi x}{a}=\rho h\ddot{u} \end{aligned} \tag{2.9}$$

Neglecting the in-plane displacements i.e. $u(t)=v(t)=0$, then from equations $(2.9)_{2,3}$, it is clear that

$$\frac{x}{a}=\frac{y}{b}=\frac{1}{2} \tag{2.10}$$

Using equation (2.10) in equation $(2.9)_1$, neglecting the in-plane displacements, and simplifying the resulting expression, the equation for lateral displacement of the trimorph plate is derived as shown in equation (2.11)

$$\ddot{w} + \overline{C}\dot{w} + \overline{D}w(t) + \overline{B}[w(t)]^2 = \overline{Q}\sin(\omega t) \tag{2.11}$$

where $w(t)$ is the time-dependent lateral displacement of the trimorph plate,

$\overline{C} = \dfrac{c}{\rho h}$ is the damping constant per unit mass,

$\overline{D} = \dfrac{\pi^4}{\rho h}\Big[\dfrac{D_{11}}{a^4} + \dfrac{2(D_{12}+2D_{66})}{a^2b^2} + \dfrac{D_{11}}{b^4}\Big]$ is the bending elastic stiffness per unit mass,

$\overline{B} = \dfrac{\pi^4}{\rho h}B_{11}\Big(\dfrac{1}{b^4} + \dfrac{1}{a^4}\Big)$ is the bending-extension elastic stiffness per unit mass,

$\overline{Q} = \dfrac{q}{\rho h}$ is the magnitude of the excitation force per unit mass.

Equation (2.11) is a nonlinear ODE which models the lateral response of a rectangular laminated plate acted upon by a sinusoidally varying and sinusoidally distributed excitation force and subjected to linear viscous damping. The nonlinearity in the equation of lateral motion of the trimorph plate is introduced by the membrane forces. This equation is different from the common Duffing's equation for nonlinear vibration because the nonlinear term has a power of two, and the equation is introduced for the first time.

If the nonlinear term is neglected, equation (2.11) reduces to

$$\ddot{w} + \overline{C}\dot{w} + \overline{D}w(t) = \overline{Q}\sin(\omega t) \tag{2.12}$$

Equation (2.12) models the linear lateral response of the same system. Equations (2.11) and (2.12) can be solved by direct integration using software packages. Bespoke Mathematica$^{\text{TM}}$ codes have been used to solve these equations and simulate graphically the time-domain and frequency-domain responses of the trimorph plate for the different layer-stacking.

3. Determination of the elastic coefficients of the trimorph plate

The response of the plate is largely dependent on the elastic stiffness of the plate. The trimorph plate stiffness is determined by $\overline{D}$ and $\overline{B}$ for the nonlinear response and just $\overline{D}$ for the linear response. From equation (2.11), $\overline{D}$ is dependent on the stiffness coefficients D_{11}, D_{12}, and D_{66} while $\overline{B}$ is dependent

on the stiffness coefficient B_{11}. A more generalised approach for the determination of the stiffness coefficients of laminates was provided by Noor and Tenek (1992). Expressions for the determination of thermoelastic coefficients and the derivatives of coefficients with respect to material properties of the laminae were developed. They also illustrated the effect of stacking sequence and fibre orientation on the coefficients and for the first time provided sensitivity derivatives. Here an attempt has been made to simplify algebraically and to present more concise equations for determining the stiffness coefficients for the trimorph plate (see appendix).

4. Numerical integration and discussion of the results

Numerical integration routines, as are found in many standard software packages, can be used to solve PDEs and ODEs directly, and Israr (2008) used the NDSolve solver in Mathematica^{TM} for the solution of the governing equation for vibration of a cracked aluminium plate. A similar approach was taken by Atepor (2008) and Ganilova and Cartmell (2010). Optimised time-domain responses have been simulated here, using the NDSolve integrator. Optimisation of the trimorph plate response involves solving the objective functions, which are equations (2.11) and (2.12), within the optimisation constraints. Two outputs have been constrained in this study to obtain an optimised response. The first constrained output is the time take for the plate response to go into steady-state as the initial response is transient. This transient behaviour, though it cannot be eliminated in reality, can only be allowed for a short period since it is not desirable and hence is the reason for constraining it. A steady-state response time of not more than thirty seconds is used here. The second constrained output is the amplitude of the steady-state response. It is desirable in many applications of vibration to keep the maximum amplitude of vibration within certain acceptable limits. This means that the response has to be constrained and for the purpose of this study, a response range of ± 10 percent of one-tenth of the plate thickness is deemed to be acceptable. The objective function and optimisation constraints are summarised as follows:

— objective functions

$$(1) \quad \ddot{w} + \overline{C}\dot{w} + \overline{D}w(t) + \overline{B}[w(t)]^2 = \overline{Q}\sin(\omega t) \qquad \text{nonlinear}$$

$$(2) \quad \ddot{w} + \overline{C}\dot{w} + \overline{D}w(t) = \overline{Q}\sin(\omega t) \qquad \text{linear}$$

— constraints

$$T_s \leqslant 30 \qquad 0.09h \leqslant [w(t)]_{opt} \leqslant 0.11h$$

where T_s is the time in seconds taken for the plate response to go into steady-state and $[w(t)]_{opt}$ is the optimum response in metres. The limit of the steady-state response time is chosen arbitrarily. As for the response limit, the normal case for small deflections of thin plates (Timoshenko and Woinowsky-Krieger, 1959) is applied, i.e. the lateral displacement is in the order of one-tenth of the plate thickness. For the purpose of simulating the temporal response of the trimorph plate, three different materials were used namely: Aluminium (Al), Polyvinylidene Fluoride (PVDF) and Lead Zirconate Titanate (PZT). Properties of these materials and other input parameters are given in Tables 1 and 2 respectively.

Table 1. Material properties of the plate layers

Material	Poisson's ratio ν [–]	Modulus E [GPa]	Density ρ [kg/m^3]
Aluminium, Al	0.33	70	2700
PVDF	0.44	1.1	1770
PZT	0.3	64	7600

The properties of PVDF were obtained from Zhang *et al.* (1993) and the website, http://www.texloc.com/closet/cl_pvdf_properties.htm while the properties of PZT were obtained from Malic *et al.* (1992) and Yimnirun *et al.* (2004).

Table 2. Other inputs used for simulating trimorph plate response

Input	Value	Unit
Length, a	2	m
Width, b	0.5	m
Thickness of Al, δ_{Al}	1	mm
Thickness of PVDF, δ_{PVDF}	0.7	mm
Thickness of PZT, δ_{PZT}	0.3	mm
Exciting force, q	10	N/m^2

From Table 2, it can be seen that a rectangular plate of unit area and total thickness of 2 mm has been chosen. Hence the thickness to length

ratio (h/L) is 1/1000, which means the plate is defined as a thin plate. Since the trimorph plate comprises of three different layers, then the stacking of the layers can be carried out in six different permutations namely: Al/PVDF/PZT, Al/PZT/PVDF, PVDF/Al/PZT, PVDF/PZT/Al, PZT/PVDF/Al, and PZT/Al/PVDF. Response plots for the different stacking arrangement are shown below.

4.1. Nonlinear time-domain response

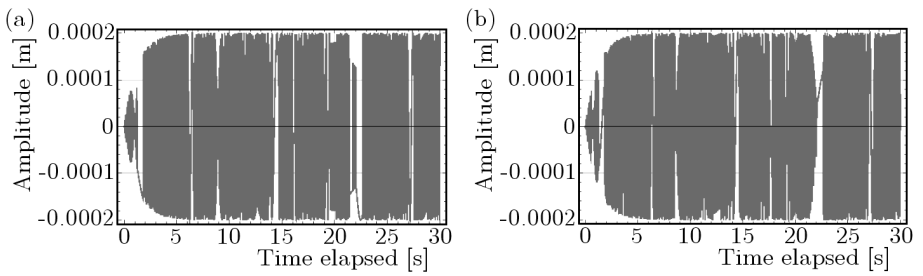

Fig. 2. Optimised time-domain response of Al/PVDF/PZT (a) and Al/PZT/PVDF (b) stacking with $\xi = 0.00018$

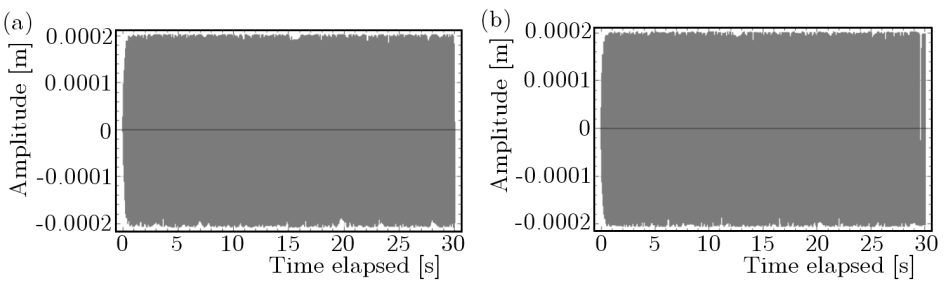

Fig. 3. Optimised time-domain response of PVDF/Al/PZT (a) and PVDF/PZT/Al (b) stacking with $\xi = 0.01$

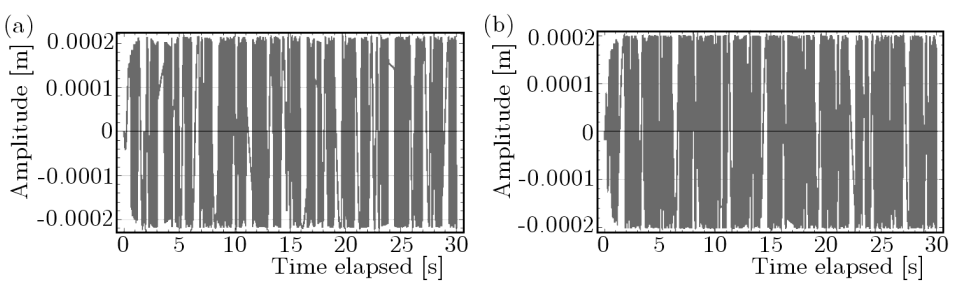

Fig. 4. Optimised time-domain response of PZT/PVDF/Al (a) and PZT/Al/PVDF (b) stacking with $\xi = 0.0022$

4.2. Linear time-domain response

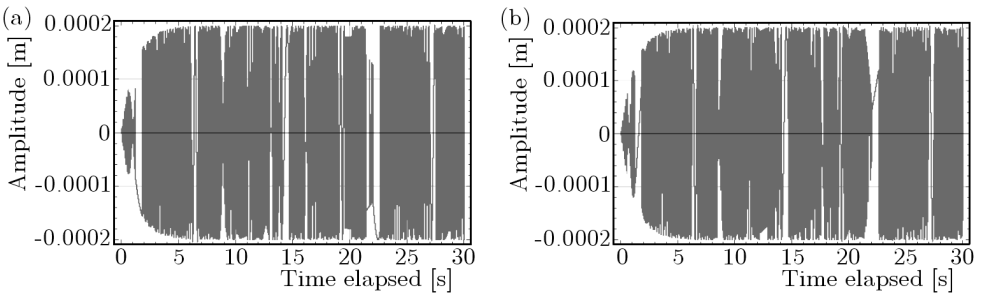

Fig. 5. Optimised time-domain response of Al/PVDF/PZT (a) and Al/PZT/PVDF (b) stacking with $\xi = 0.00018$

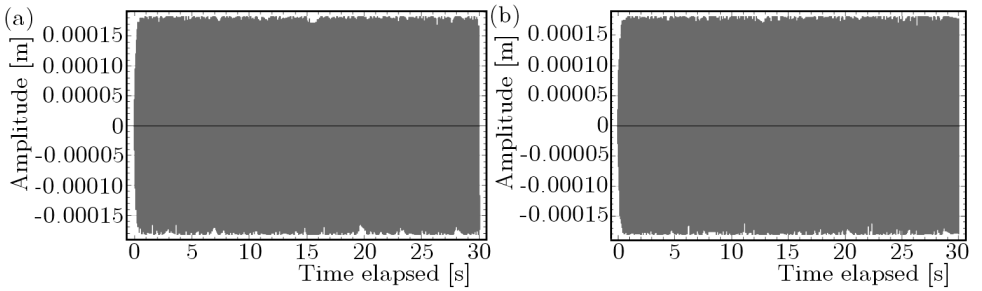

Fig. 6. Optimised time-domain response of PVDF/Al/PZT (a) and PVDF/PZT/Al (b) stacking with $\xi = 0.018$

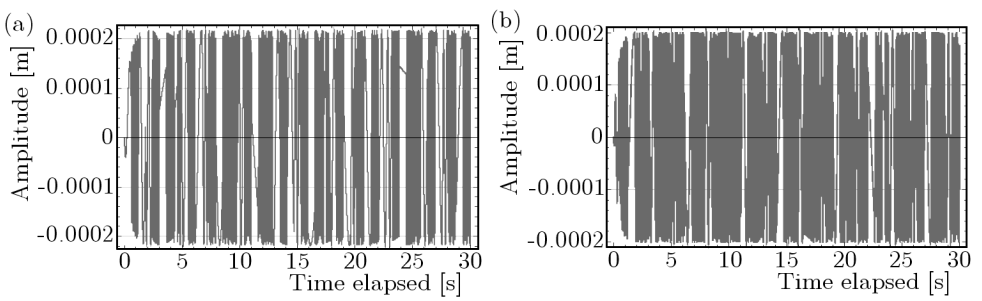

Fig. 7. Optimised time-domain response of PZT/PVDF/Al (a) and PZT/Al/PVDF (b) stacking with $\xi = 0.0022$

In simulating the optimised response to satisfy the optimisation constraints, the damping of the system was varied by varying the damping ratio. This was so because for a given set of layer thicknesses and in-plane dimensions, the plate stiffnesses ($\overline{D}$ and $\overline{B}$) cannot be altered to satisfy the optimisation constraints, therefore leaving only the option of varying the damping constant $\overline{C}$,

which can easily be done through the damping ratio ξ. The results obtained from simulating the optimised response of the trimorph plate for the different layer-stacking are summarised in Table 3 and 4 for the nonlinear and linear analysis respectively.

Table 3. Nonlinear analysis of the trimorph plate response for the different layer arrangement

S/N	Layer arrangem. 1-2-3 respectively	Plate density [kg/m^3]	Plate stiffness (B) [N/mkg]	Plate stiffness (BE) [N/m^{2}kg]	Operating freq. [rad/s]	Damping const. [Ns/mkg]	Steady-state response [m]	Steady-state set-in time [s]
1	Al/PVDF/PZT	3109.50	$2.229 \cdot 10^7$	$2.006 \cdot 10^7$	4721.08	1.700	$2.004 \cdot 10^{-4}$	6
2	Al/PZT/PVDF	3109.50	$2.228 \cdot 10^7$	$1.641 \cdot 10^7$	4719.77	1.699	$2.005 \cdot 10^{-4}$	6
3	PVDF/Al/PZT	3109.50	$2.439 \cdot 10^5$	$3.367 \cdot 10^7$	493.83	9.877	$2.040 \cdot 10^{-4}$	3
4	PVDF/PZT/Al	3109.50	$2.458 \cdot 10^5$	$3.430 \cdot 10^7$	495.74	9.915	$2.024 \cdot 10^{-4}$	3
5	PZT/PVDF/Al	3109.50	$1.846 \cdot 10^6$	$3.067 \cdot 10^7$	1358.64	5.435	$2.175 \cdot 10^{-4}$	3
6	PZT/Al/PVDF	3109.50	$1.811 \cdot 10^6$	$1.703 \cdot 10^7$	1345.61	5.921	$2.017 \cdot 10^{-4}$	3

B denotes bending stiffness while BE denotes bending-extension stiffness

Table 4. Linear analysis of the trimorph plate response for the different layer arrangement

S/N	Layer arrangem. 1-2-3 respectively	Plate density [kg/m^3]	Plate stiffness (B) [N/mkg]	Natural freq. [rad/s]	Damping const. [Ns/mkg]	Steady-state response [m]	Steady-state set-in time [s]
1	Al/PVDF/PZT	3109.50	$2.229 \cdot 10^7$	4721.08	1.700	$2.003 \cdot 10^{-4}$	6
2	Al/PZT/PVDF	3109.50	$2.228 \cdot 10^7$	4719.77	1.699	$2.005 \cdot 10^{-4}$	6
3	PVDF/Al/PZT	3109.50	$2.439 \cdot 10^5$	493.83	17.778	$1.831 \cdot 10^{-4}$	3
4	PVDF/PZT/Al	3109.50	$2.458 \cdot 10^5$	495.74	17.847	$1.817 \cdot 10^{-4}$	3
5	PZT/PVDF/Al	3109.50	$1.846 \cdot 10^6$	1358.64	5.435	$2.178 \cdot 10^{-4}$	3
6	PZT/Al/PVDF	3109.50	$1.811 \cdot 10^6$	1345.61	5.921	$2.012 \cdot 10^{-4}$	3

Tables 3 and 4 provide a comprehensive summary of the results obtained from simulating the time-domain responses of the different layer-stacking for nonlinear and linear analysis respectively. It can be observed from column three of both tables that the density of the trimorph plate is not affected by different layer-stacking since the material properties and layer thicknesses are unchanged. The last column of the tables shows when the steady-state

response develops noticeably and definitively. It can be seen from the tables that the steady-state response was achieved in less than 10 seconds in all cases.

The results also reveal that the responses for rows 1 and 2 are similar. So also are rows 3 and 4 and rows 5 and 6. The implication is that the response is dependent on the first layer (layer 1), which is called the *reference layer* in this study. The reference layer is the layer directly experiencing the lateral load and could be either of the top-most or bottom-most layer. This reduces the problem of optimising the trimorph plate response to simulating only three different configurations instead of the six possible configurations. The optimised responses of the three necessary configurations are given in rows 1, 3 and 5.

In determining the best possible layer-stacking from the three configurations necessary for testing/simulation, the trimorph plate stiffness, natural frequency and damping coefficient (or ratio) are worth considering. It is required for most applications, for example in damage mitigation, to use a material with high resilience to load. Also, a better material would have a high natural frequency to avoid the occurrence of resonance in operation and would require lower damping to reduce the cost of vibration and noise control. From the nonlinear analysis (Table 3) it can be seen that row 1 has the best combination of these considerations compared to rows 3 and 5. It is important that the nonlinearity in the response is minimised as much as possible. Although, row 2 has the least value for the coefficient of the nonlinear term (bending-extension stiffness coefficient), row 1 still produces the best response characteristics after considering the other factors discussed above. Row 1 has the highest bending stiffness (22.289 MN/mkg), the highest natural frequency (4721.00 rad/s = 751.29 Hz – This value is obtained from the nonlinear frequency-domain response plot of the configuration Al/PVDF/PZT) and the second lowest damping (1.700 Ns/mkg). Similarly, from the linear analysis (Table 4) row 1 has the best combination of response characteristics as follows: bending stiffness = 22.289 MN/mkg, natural frequency = 4721.08 rad/s = 751.29 Hz, and damping constant = 1.700 Ns/mkg. Hence, it can be concluded that the configuration with the best dynamic response is either of Al/PVDF/PZT or Al/PZT/PVDF since both give very similar responses.

4.3. Frequency-domain response

The frequency-domain (FD) plots for nonlinear and linear responses have been simulated under identical condition i.e. the same magnitude of force, damping factor, in-plane dimensions and materials. The FD plots (Figs. 8 to 13) reveal approximately equal responses for Al/PVDF/PZT and Al/PZT/PVDF

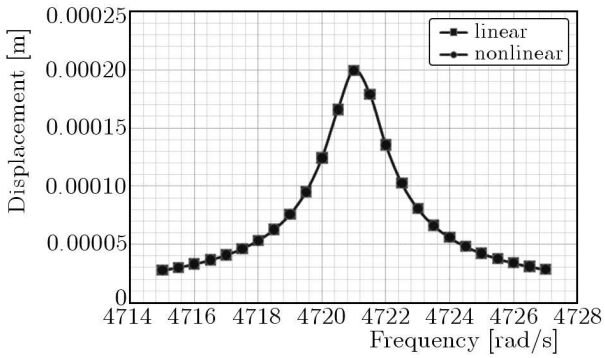

Fig. 8. Frequency-domain response of Al/PVDF/PZT trimorph plate configuration

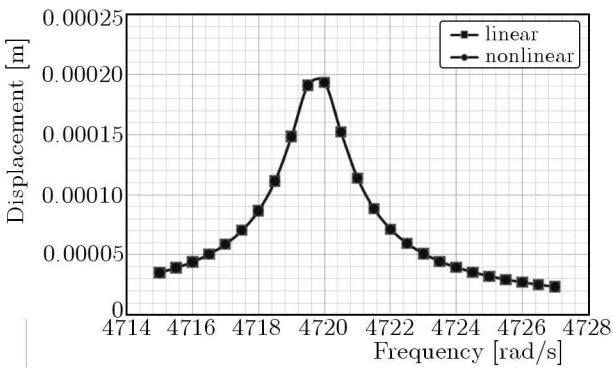

Fig. 9. Frequency-domain response of Al/PZT/PVDF trimorph plate configuration

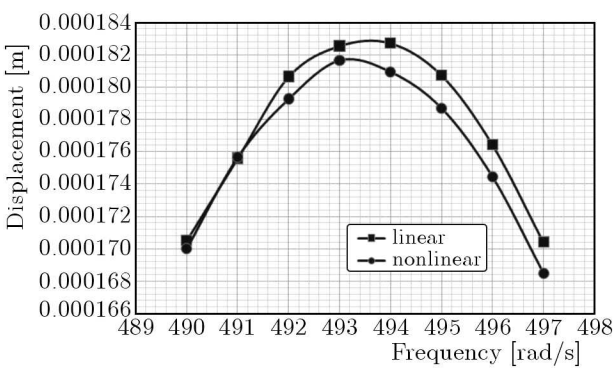

Fig. 10. Frequency-domain response of PVDF/Al/PZT trimorph plate configuration

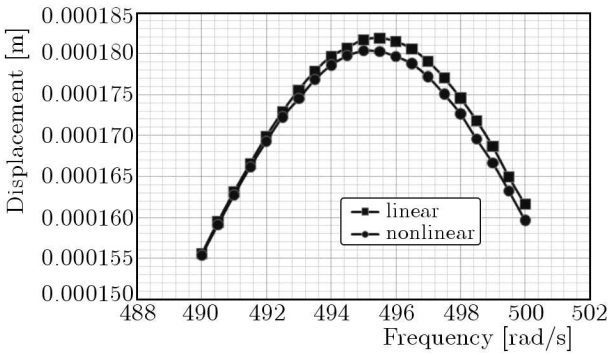

Fig. 11. Frequency-domain response of PVDF/PZT/Al trimorph plate configuration

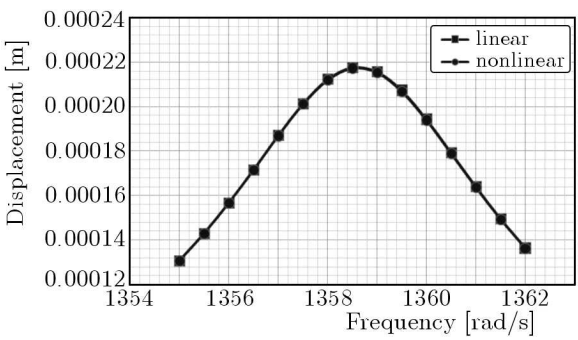

Fig. 12. Frequency-domain response of PZT/PVDF/Al trimorph plate configuration

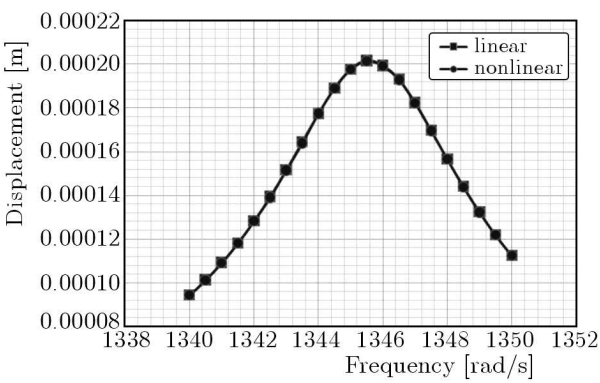

Fig. 13. Frequency-domain response of PZT/Al/PVDF trimorph plate configuration

trimorph configurations, slight difference in the responses for PVDF/Al/PZT and PVDF/PZT/Al trimorph configurations, and approximately equal responses for PZT/PVDF/Al and PZT/Al/PVDF trimorph. The plots also show that the peak response for the linear analysis is higher than the peak response for the corresponding nonlinear analysis in the cases where there are differences. Also, in the cases were the linear and nonlinear responses differ, the natural frequency of the linear response is higher than the corresponding natural frequency of the nonlinear response (Table 5). Hence, it is concluded that the effect of the nonlinear term in the equation of motion is such as to reduce the natural frequency of the trimorph plate and this is expected in principle. Although, the reduction in natural frequency as shown in Table 5 is not large, it is believed that this reduction can be quite significant depending on the dimensions of and the materials for the trimorph plate.

Frequency-domain plots have been produced using the same system inputs for both analyses in order to compare the nonlinear and linear responses. The plots are shown in Figs. 8 to 13 below.

Table 5. Comparison of natural frequencies for linear and nonlinear response obtained from frequency-domain plots

S/N	Layer arrangement 1-2-3 respectively	Linear response [rad/s]	Nonlinear response [rad/s]
1	Al/PVDF/PZT	4721.0	4721.0
2	Al/PZT/PVDF	4719.8	4719.8
3	PVDF/Al/PZT	493.2	493.7
4	PVDF/PZT/Al	495.2	495.6
5	PZT/PVDF/Al	1358.6	1358.6
6	PZT/Al/PVDF	1345.6	1345.6

Table 5 summarises the natural frequencies of the nonlinear and linear responses obtained from the frequency-domain plots for the different layer-stacking of the trimorph plate.

5. Conclusions

The dynamics of a trimorph plate have been investigated in this paper. The trimorph plate is a three-layer laminated plate with each layer made of a different material. The plate is subjected to a sinusoidally distributed and varying load and a linear viscous damping force.

In studying the trimorph plate, the governing equations for deformation of the plate were developed using the classical plate theory and classical laminate theory as in equations (2.7). The governing equations were reduced to ordinary differential equations (ODEs) as in equations (2.11) and (2.12) for modelling the lateral deformation of the trimorph plate using the Navier method. The ODEs were used to simulate the time-domain and frequency-domain responses of the plate by direct integration using bespoke Mathematica^{TM} code. The time-domain plots revealed that the responses were initially transient and settled into steady-state after some time. To optimise the responses, the steady-state commencement time was constrained to 30 seconds and the acceptable maximum deflection at steady-state was constrained to ± 10 percent of one-tenth the thickness of the plate. The materials used to simulate the trimorph plate responses were aluminium (Al), polyvinylidene fluoride (PVDF) and lead zirconate titanate (PZT). From the response simulations, it was discovered that only three out of the six possible different layer-stacking is necessary to determine the best stacking for the trimorph plate. Considering the trimorph plate stiffness, fundamental natural frequency and damping coefficient, either one of the Al/PVDF/PZT or AL/PZT/PVDF configurations was found to produce the best response given that both stackings produced very similar responses.

Frequency-domain response plots were also generated for the nonlinear and linear responses for the purpose of comparison. Frequency-domain responses were generated over a chosen frequency interval, and the data were plotted. The plots reveal that for configurations in which the nonlinear effect was significant, the peak response and the natural frequency of the nonlinear response are lower than that of the corresponding linear response for the same system inputs. Therefore, the plots show that nonlinearity in the responses acts to reduce the natural frequency of the trimorph plate.

This study has been limited to a rectangular trimorph plate that has isotropic layers subjected to a sinusoidally distributed load and is simply-supported on all four edges. This leaves room for further investigation of other loading and boundary conditions. It is intended that the results obtained here will be validated experimentally and numerically using software packages such as ABAQUS. This study can be applied to the study of optimised damage mitigation in structures subjected to potentially dangerous loads by considering one of the layers of the trimorph configuration as the host material, one as the sensor and the other as the actuator, and using the vibration analysis above to determine what arrangement of the layers will produce the best structural integrity under the operating constraints of the material.

A. Appendix

The stiffness coefficients for the trimorph plate have been presented in a simplified form based on the geometry of the layers. In order to accomplish this, the reference layer labelled layer 1 is an outer layer as shown in Fig. 14. The reference layer is the layer directly experiencing the lateral load and could be either of the top-most or bottom-most layer, but for the purpose of illustration the bottom-most layer is used. Other layers are labelled accordingly as shown in Fig. 14.

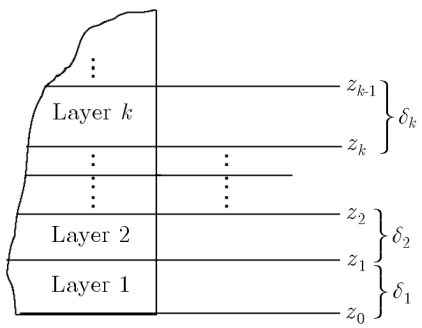

Fig. 14. Sketch illustrating vertical deometry of laminae

From Fig. 14, the following can be deduced geometrically

$$\begin{aligned} z_k - z_{k-1} &= \delta_k \\ z_k &= \sum_{i=1}^{k} \delta_i \qquad k > 0 \quad \text{or} \\ z_{k-1} &= \sum_{i=1}^{k-1} \delta_i \qquad k > 1 \quad \text{else} \quad z_{k-1} = 0 \end{aligned} \tag{A.1}$$

where δ_k is the thickness of the kth layer and $k = 1, 2, 3$.

A_{ij} coefficients

For the kth layer, $(A_{ij})_k = (\overline{Q}_{ij})_k (z_k - z_{k-1}) = (\overline{Q}_{ij})_k \delta_k$.
So that

$$\begin{aligned} (A_{11})_k &= (\overline{Q}_{11})_k \delta_k = \frac{E_k}{1-\nu_k^2}\delta_k \\ (A_{12})_k &= (\overline{Q}_{12})_k \delta_k = \frac{\nu_k E_k}{1-\nu_k^2}\delta_k \\ (A_{66})_k &= (\overline{Q}_{66})_k \delta_k = \frac{E_k}{2(1+\nu_k)}\delta_k \end{aligned} \tag{A.2}$$

where $k = 1, 2, 3$ for layer 1, layer 2 and layer 3, respectively.

Hence, the extensional stiffness coefficients are given by

$$
\begin{aligned}
A_{11} &= \sum_{i=1}^{k}(A_{11})_k = \frac{E_1}{1-\nu_1^2}\delta_1 + \frac{E_2}{1-\nu_2^2}\delta_2 + \frac{E_3}{1-\nu_3^2}\delta_3 \\
A_{12} &= \sum_{i=1}^{k}(A_{12})_k = \frac{\nu_1 E_1}{1-\nu_1^2}\delta_1 + \frac{\nu_2 E_2}{1-\nu_2^2}\delta_2 + \frac{\nu_3 E_3}{1-\nu_3^2}\delta_3 \\
A_{66} &= \sum_{i=1}^{k}(A_{66})_k = \frac{1}{2}\Big(\frac{E_1}{1+\nu_1}\delta_1 + \frac{E_2}{1+\nu_2}\delta_2 + \frac{E_3}{1+\nu_3}\delta_3\Big)
\end{aligned}
\tag{A.3}
$$

$\underline{B_{ij}}$ coefficients

For the kth layer, $(B_{ij})_k = (\overline{Q}_{ij})_k(z_k^2 - z_{k-1}^2)$,
$z_k^2 - z_{k-1}^2 = (z_k + z_{k-1})(z_k - z_{k-1})$.

Substituting equations (A.1),
$z_k^2 - z_{k-1}^2 = (\delta_k + 2z_{k-1})\delta_k = \delta_k(\delta_k + 2\sum_{i=1}^{k-1}\delta_i$.

Therefore, $(B_{ij})_k = (\overline{Q}_{ij})_k\delta_k(\delta_k + 2\sum_{i=1}^{k-1}\delta_i)$.

So that,

— for layer 1 $(k = 1)$

$$
\begin{aligned}
(B_{11})_1 &= (\overline{Q}_{11})_k\delta_1^2 = \frac{E_1}{1-\nu_1^2}\delta_1^2 \\
(B_{12})_1 &= (\overline{Q}_{12})_1\delta_1^2 = \frac{\nu_1 E_1}{1-\nu_1^2}\delta_1^2 \\
(B_{66})_1 &= (\overline{Q}_{66})_1\delta_1^2 = \frac{E_1}{2(1+\nu_1)}\delta_1^2
\end{aligned}
\tag{A.4}
$$

— for layer 2 $(k = 2)$, $(B_{ij})_2 = (\overline{Q}_{ij})_2\delta_2(\delta_2 + 2\delta_1)$

$$
\begin{aligned}
(B_{11})_2 &= (\overline{Q}_{11})_2\delta_2(\delta_2 + 2\delta_1) = \frac{E_2}{1-\nu_2^2}\delta_2(\delta_2 + 2\delta_1) \\
(B_{12})_2 &= (\overline{Q}_{12})_2\delta_2(\delta_2 + 2\delta_1) = \frac{\nu_2 E_2}{1-\nu_2^2}\delta_2(\delta_2 + 2\delta_1) \\
(B_{66})_2 &= (\overline{Q}_{66})_2\delta_2(\delta_2 + 2\delta_1) = \frac{E_2}{2(1+\nu_2)}\delta_2(\delta_2 + 2\delta_1)
\end{aligned}
\tag{A.5}
$$

— for layer 3 $(k=3)$, $(B_{ij})_3 = (\overline{Q}_{ij})_3\delta_3[\delta_3 + 2(\delta_2+\delta_1)]$

$$\begin{aligned}
(B_{11})_3 &= (\overline{Q}_{11})_3\delta_3[\delta_3 + 2(\delta_2+\delta_1)] = \frac{E_3}{1-\nu_3^2}\delta_3[\delta_3 + 2(\delta_2+\delta_1)] \\
(B_{12})_3 &= (\overline{Q}_{12})_3\delta_3[\delta_3 + 2(\delta_2+\delta_1)] = \frac{\nu_3 E_3}{1-\nu_3^2}\delta_3[\delta_3 + 2(\delta_2+\delta_1)] \\
(B_{66})_3 &= (\overline{Q}_{66})_3\delta_3[\delta_3 + 2(\delta_2+\delta_1)] = \frac{E_3}{2(1+\nu_3)}\delta_3[\delta_3 + 2(\delta_2+\delta_1)]
\end{aligned} \tag{A.6}$$

Hence, the bending-extension stiffness coefficients are given by

$$\begin{aligned}
B_{11} &= \frac{1}{2}\sum_{i=1}^{k}(B_{11})_k \\
&= \frac{1}{2}\Big(\frac{E_1}{1-\nu_1^2}\delta_1^2 + \frac{E_2}{1-\nu_2^2}\delta_2(\delta_2+2\delta_1) + \frac{E_3}{1-\nu_3^2}\delta_3[\delta_3+2(\delta_2+\delta_1)]\Big) \\
B_{12} &= \frac{1}{2}\sum_{i=1}^{k}(B_{12})_k \\
&= \frac{1}{2}\Big(\frac{\nu_1 E_1}{1-\nu_1^2}\delta_1^2 + \frac{\nu_2 E_2}{1-\nu_2^2}\delta_2(\delta_2+2\delta_1) + \frac{\nu_3 E_3}{1-\nu_3^2}\delta_3[\delta_3+2(\delta_2+\delta_1)]\Big) \\
B_{66} &= \frac{1}{2}\sum_{i=1}^{k}(B_{66})_k \\
&= \frac{1}{4}\Big(\frac{E_1}{1+\nu_1}\delta_1^2 + \frac{E_2}{1+\nu_2}\delta_2(\delta_2+2\delta_1) + \frac{E_3}{1+\nu_3}\delta_3[\delta_3+2(\delta_2+\delta_1)]\Big)
\end{aligned} \tag{A.7}$$

$\underline{D_{ij} \text{ coefficients}}$

For each layer, $(D_{ij})_k = (\overline{Q}_{ij})_k(z_k^3 - z_{k-1}^3)$,
$z_k^3 - z_{k-1}^3 = (z_k - z_{k-1})^3 + 3(z_k - z_{k-1})z_k z_{k-1} = \delta_k^3 + 3\delta_k \sum_{i=1}^{k}\delta_i \sum_{i=1}^{k-1}\delta_i$.

Therefore, $(D_{ij})_k = (\overline{Q}_{ij})_k(\delta_k^3 + 3\delta_k)\sum_{i=1}^{k}\delta_i \sum_{i=1}^{k-1}\delta_i$
— for layer 1 $(k=1)$, $(D_{ij})_1 = (\overline{Q}_{ij})_1(\delta_1^3 + 3\delta_1^2)$

$$\begin{aligned}
(D_{11})_1 &= (\overline{Q}_{11})_1(\delta_1^3 + 3\delta_1^2) = \frac{E_1}{1-\nu_1^2}(\delta_1^3 + 3\delta_1^2) \\
(D_{12})_1 &= (\overline{Q}_{12})_1(\delta_1^3 + 3\delta_1^2) = \frac{\nu_1 E_1}{1-\nu_1^2}(\delta_1^3 + 3\delta_1^2) \\
(D_{66})_1 &= (\overline{Q}_{66})_1(\delta_1^3 + 3\delta_1^2) = \frac{E_1}{2(1+\nu_1)}(\delta_1^3 + 3\delta_1^2)
\end{aligned} \tag{A.8}$$

— for layer 2 $(k=2)$, $(D_{ij})_2 = (\overline{Q}_{ij})_2[\delta_2^3 + 3\delta_2\delta_1(\delta_1+\delta_2)]$

$$
\begin{aligned}
(D_{11})_2 &= (\overline{Q}_{11})_2[\delta_2^3 + 3\delta_2\delta_1(\delta_1+\delta_2)] = \frac{E_2}{1-\nu_2^2}[\delta_2^3 + 3\delta_2\delta_1(\delta_1+\delta_2)] \\
(D_{12})_2 &= (\overline{Q}_{12})_2[\delta_2^3 + 3\delta_2\delta_1(\delta_1+\delta_2)] = \frac{\nu_2 E_2}{1-\nu_2^2}[\delta_2^3 + 3\delta_2\delta_1(\delta_1+\delta_2)] \\
(D_{66})_2 &= (\overline{Q}_{66})_2[\delta_2^3 + 3\delta_2\delta_1(\delta_1+\delta_2)] = \frac{E_2}{2(1+\nu_2)}[\delta_2^3 + 3\delta_2\delta_1(\delta_1+\delta_2)]
\end{aligned}
\tag{A.9}
$$

— for layer 3 $(k=3)$, $(D_{ij})_3 = (\overline{Q}_{ij})_3[\delta_3^3 + 3\delta_3(\delta_1+\delta_2)(\delta_1+\delta_2+\delta_3)]$

$$
\begin{aligned}
(D_{11})_3 &= (\overline{Q}_{11})_3[\delta_3^3 + 3\delta_3(\delta_1+\delta_2)(\delta_1+\delta_2+\delta_3)] \\
&= \frac{E_3}{1-\nu_3^2}[\delta_3^3 + 3\delta_3(\delta_1+\delta_2)(\delta_1+\delta_2+\delta_3)] \\
(D_{12})_3 &= (\overline{Q}_{12})_3[\delta_3^3 + 3\delta_3(\delta_1+\delta_2)(\delta_1+\delta_2+\delta_3)] \\
&= \frac{\nu_3 E_3}{1-\nu_3^2}[\delta_3^3 + 3\delta_3(\delta_1+\delta_2)(\delta_1+\delta_2+\delta_3)] \\
(D_{66})_3 &= (\overline{Q}_{66})_3[\delta_3^3 + 3\delta_3(\delta_1+\delta_2)(\delta_1+\delta_2+\delta_3) \\
&= \frac{E_3}{2(1+\nu_3)}[\delta_3^3 + 3\delta_3(\delta_1+\delta_2)(\delta_1+\delta_2+\delta_3)]
\end{aligned}
\tag{A.10}
$$

Hence, the bending stiffness coefficients are given by

$$
\begin{aligned}
D_{11} &= \frac{1}{3}\sum_{i=1}^{k}(D_{11})_k = \frac{1}{3}\Big(\frac{E_1}{1-\nu_1^2}(\delta_1^3 + 3\delta_1^2) \\
&\quad + \frac{E_2}{1-\nu_2^2}[\delta_2^3 + 3\delta_2\delta_1(\delta_1+\delta_2)] + \frac{E_3}{1-\nu_3^2}[\delta_3^3 + 3\delta_3(\delta_1+\delta_2)(\delta_1+\delta_2+\delta_3)]\Big) \\
D_{12} &= \frac{1}{3}\sum_{i=1}^{k}(D_{12} = \frac{1}{3}\Big(\frac{\nu_1 E_1}{1-\nu_1^2}(\delta_1^3 + 3\delta_1^2) \\
&\quad + \frac{\nu_2 E_2}{1-\nu_2^2}[\delta_2^3 + 3\delta_2\delta_1(\delta_1+\delta_2)] + \frac{\nu_3 E_3}{1-\nu_3^2}[\delta_3^3 + 3\delta_3(\delta_1+\delta_2)(\delta_1+\delta_2+\delta_3)]\Big) \\
D_{66} &= \frac{1}{3}\sum_{i=1}^{k}(D_{66})_k = \frac{1}{6}\Big(\frac{E_1}{1+\nu_1}(\delta_1^3 + 3\delta_1^2) \\
&\quad + \frac{E_2}{1+\nu_2}[\delta_2^3 + 3\delta_2\delta_1(\delta_1+\delta_2)] + \frac{E_3}{1+\nu_3}[\delta_3^3 + 3\delta_3(\delta_1+\delta_2)(\delta_1+\delta_2+\delta_3)]\Big)
\end{aligned}
\tag{A.11}
$$

References

1. Atepor L., 2008, Vibration analysis and intelligent control of flexible rotor systems using smart materials, PhD Thesis, Department of Mechanical Engineering, University of Glasgow, UK
2. Chang S., Lin J., 2003, Analysis and optimisation of trimorph ring transducers, *Journal of Vibration and Sound*, **263**, 831-851
3. Craciunescu C.M., Mihalca I., Budau V., 2005, Trimorph actuation based on shape memory alloys, *Journal of Optoelectronics and Advanced Materials*, **7**, 2, 1113-1120
4. Erturk A., Inman D.J., 2009, Electromechanical modelling of cantilevered piezoelectric energy harvesters for persistent base motions, [In:] *Energy Harvesting Technologies*, Priya S. and Inman D.J. (Eds), Springer, New York
5. Ganilova O.A., Cartmell M.P., 2010, An analytical model for the vibration of a composite plate containing an embedded periodic shape memory alloy structure, *Composites Structures*, **92**, 39-47
6. Israr A., 2008, Vibration analysis of cracked aluminium plates, PhD Thesis, Department of Mechanical Engineering, University of Glasgow, UK
7. Jones R.M., 1999, *Mechanics of Composite Materials*, 2nd Edition, Taylor and Francis, Philadelphia
8. Lee C.K., 1990, Theory of laminated piezoelectric plates for the design of distributed sensors/actuators. Part I: Governing equations and reciprocal relationships, *Journal of Acoustical Society of America*, **87**, 3, 1144-1158
9. Liew K.M., He X.Q., Tan M.J., Lim H.K., 2004, Dynamic analysis of laminated composite plates with piezoelectric sensor/actuator patches using the FSDT mesh-free method, *International Journal of Mechanical Sciences*, **46**, 411-431
10. Lu H., Li J., 2009, Analysis of an initially stressed laminated plate based on elasticity theory, *Composite Structures*, **88**, 271-279
11. Malic B., Kosec M., Kosmac T., 1992, Mechanical and electric properties of PZT-ZrO_2 composites, *Ferroelectrics*, **129**, 2, 147-155
12. Noor A.K., Tenek L.H., 1992, Stiffness and thermoelastic coefficients of composite laminates, *Composite Structures*, **21**, 57-66
13. Papilla M., Sheplak M., Cattafesta III L.N., 2008, Optimisation of clamped circular piezoelectric composite actuators, *Sensors and Actuators A*, **147**, 310-323
14. Reddy J.N., 2004, *Mechanics of Laminated Composite Plates and Shells: Theory and Analysis*, 2nd Edition, CRC Press, Boca Raton

15. ROYTBURD A.L., KIM T.S., SU Q., SLUTSKER J., WUTTIG M., 1998, Martensitic transformation in constrained films, *Acta Materialia*, **46**, 14, 5095-5107

16. The TexLoc Closet, 2005, PVDF Detailed Properties (Polyvinylidene Fluoride), Parker-Texloc, Texas, [Online] Accessed at: http://www.texloc.com/closet/cl_pvdf_properties.htm, Accessed: July 2010

17. TIMOSHENKO S., WOINOWSKY-KRIEGER S., 1959, *Theory of Plates and Shells*, 2nd Edition, McGraw-Hill, New York, pp. 47, 79

18. VINSON J.R., SIERAKOWSKI R.L., 2004, *The Behaviour of Structures Composed of Composite Materials*, 2nd Edition, Kluwer Academic Publishers, New York

19. VOYIADJIS G.Z., KATTAN P.I., 2005, *Mechanics of Composite Materials with MATLAB*, Springer, Berlin Heidelberg

20. WHITNEY J.M., 1987, *Structural Analysis of Laminated Anistropic Plates*, Technomic Publishing Co. Inc., Lancaster

21. YIMNIRUN R., MEECHOWAS E., ANANTA S., TUNKASIRI T., 1992, Mechanical properties of xPMN-(1-x)PZT ceramic systems, *Chiang Mai University Journal*, **32**, 2, 147-154

22. ZAK A.J., CARTMELL M.P., OSTACHOWICZ W., 2003, Dynamics of multilayered composite plates with shape memory alloy wire, *Journal of Applied Mechanics*, **70**, 313-327

23. ZENKOUR A.M., 2004, Analytical solution for bending of cross-ply laminated plates under thermo-mechanical load, *Composite Structures*, **65**, 367-379

24. ZHANG H., GALEA S.C., CHIU W.K., LAM Y.C., 1993, An investigation of thin PVDF films as fluctuating-strain-measuring and damage-monitoring devices, *Smart Material Structures*, **2**, 206-216

Analiza drgań płyty trimorficznej pod kątem zoptymalizowanej ochrony przed uszkodzeniem

Streszczenie

Przedstawiono badania dotyczące wiskotycznie tłumionej płyty trimorficznej poddanej sinusoidalnie rozłożonemu obciążeniu przy warunkach brzegowych typu swobodne podparcie. Wyprowadzono równanie ruchu płyty, pierwszy raz w tym artykule, opisujące nieliniowy efekt ugięcia na podstawie klasycznej teorii płyt (CPT) oraz klasycznej teorii laminatów (CLT). Równanie to rozwiązano metodą Naviera oraz bezpośrednim całkowaniem numerycznym. Zoptymalizowane wykresy odpowiedzi czasowych płyty wykonanej z aluminium (Al), polifluorku winylidenu (PVDF) oraz spieków cyrkonu i tytanu (PZT) wykazały, że tylko trzy z możliwych sześciu

konfiguracji warstw trimorfu wystarczają do określenia najlepszego ułożenia warstw. Przy znajdowaniu najlepszej aranżacji warstw pod kątem zoptymalizowanej odpowiedzi dynamicznej płyty wzięto pod uwagę trzy czynniki: sztywność, częstość własną i stałą tłumienia. W tym kontekście najlepsze okazały się konfiguracje Al/PVDF/PZT oraz Al/PZT/PVDF – uzyskały najwyższą sztywność, największą częstość drgań własnych i najmniejszy współczynnik tłumienia. Wykresy otrzymane w dziedzinie częstości pozwoliły na porównanie odpowiedzi układu nieliniowego i zlinearyzowanego, ujawniając, zgodnie z przewidywaniami, że efekt nieliniowy zmniejsza częstość własną trimorfu. Wykazano także, że zaprezentowane badania mogą zostać zastosowane do analizy „inteligentnych" nadwozi samochodowych celującej w zoptymalizowane właściwości ze względu na ochronę przed uszkodzeniami oraz do krytycznych elementów bezpieczeństwa narażonych na potencjalne ryzyko zniszczenia.

Manuscript received February 4, 2011; accepted for print April 27, 2011